Low-cost monochromatic microsecond flash microbeam apparatus for single-cell photolysis of rhodopsin or other photolabile pigments

Jack M. Sullivan[a)]
Department of Ophthalmology, University of Michigan, Ann Arbor, Michigan
and Departments of Ophthalmology and Biochemistry/Molecular Biology, SUNY Health Science Center, Syracuse, New York 13210

(Received 26 August 1997; accepted for publication 23 September 1997)

Delivery of intense, brief flashes of monochromatic light are required in single-cell physiological experiments to photolyze cellular chromophores or pigments. In the xenon flash instrument constructed, flashes are collimated, made monochromatic with selectable bandpass filters and imaged into a small-core fiber. The flash is transmitted over meters to the epiflourescent port of a microscope where additional optics again collimate the beam. The objective lens of the microscope functions to condense flash energy into a microbeam in the specimen (field) plane and to image the cell under parafocal conditions. Spot diameters are 228 and 166 μm (full width half maximum) for 40× and 60× objectives. Flash intensities can be measured with this instrument during experiments using the microscope phase/differential interference contrast condenser to couple the microbeam to a calibrated photodiode. Flash intensities between 10^8 and 10^9 photons/μm^2 were achieved across the near-ultraviolet/visible spectrum. Flash durations were under 20 μs with a short-arc 7 J flash tube. Shielding and fiber transfer permit delivery of intense flashes without electromagnetic noise to the electrophysiological recording apparatus. Flashes generated with this instrument activated intramolecular charge motions (early receptor currents) in the visual pigment, rhodopsin, expressed from transgenes in single cultured cells. © *1998 American Institute of Physics.*
[S0034-6748(97)04112-9]

I. INTRODUCTION

Light flashes can be delivered to cells in the specimen plane of the light microscope either through the regular condenser or the objective lens acting as a microbeam condenser. Flash spot sizes are much larger when generated with the microscope condenser versus an objective lens (microbeam) condenser. With efficient geometric delivery systems high intensity microbeams can be imaged using lower energy and necessarily smaller flashtube sources.

A. Previous microbeam devices

Microscope devices have been previously described to generate microbeams at the cell plane using objective lenses. These instruments presented constant as opposed to transient light pulses and were used for inactivation of particular structures in cells using ultraviolet light[1–6] or during patch clamp experiments to inactivate ion channel proteins.[7] In these studies the total (inactivating) light energy delivered was critical but not its temporal presentation. That is, the preparation integrated the stimulus. These studies demonstrated that light delivered through the epiflourescent port of a microscope to an objective lens could be used to generate microbeams.[6] In addition fiber-optic delivery could be used to deliver light of sufficient intensity to inactivate proteins in functional molecular assays.[7] Although electromechanical shutters were attached to such units to impose temporal control of presentation, technical limits prevented light presentations of less that a few milliseconds.[8] Microbeam devices using flashlamps or continuous lamps or lasers with a shutter were similar in principle to the device described here but delivered only ultraviolet light of millisecond order pulse duration.[9,10]

B. The experimental problem: Time-resolved activation studies of rhodopsin

The particular experimental need was an instrument to deliver high intensity, monochromatic light flashes to single mammalian cells. These cells are made to express human opsin that was regenerated with the 11-cis-retinal (11cRet) chromophore to form rhodopsin. Rhodopsin is the visual pigment of the rod photoreceptor in the retina. 11cRet enters the chromophore pocket of opsin and forms a protonated Schiff base with lysine-296 in the seventh helix of the opsin protein.[11] We are conducting structure/function studies of the effects of engineered mutations in the human opsin gene on the activation of the visual pigment by light. The patch clamp technique[12] is used to enter single cells expressing opsin with microelectrodes gigaohm-sealed to the plasma membrane. After regeneration of the visual pigment, bright flash photolysis activates rhodopsin. The conformational transitions of rhodopsin lead to electrical charge redistribution in the membrane in which the visual pigment is oriented. We record this conformational activation current of rhodopsin, or early receptor current (ERC), on a submillisecond

a)Address correspondence to: SUNY Health Science Center at Syracuse, Dept of Biochemistry, Weiskotten Hall, Rm. 4255, 750 East Adams St. Syracuse, NY 13210; electronic mail: Sullivaj@vax.cs.hscsyr.edu

time frame from single cells expressing less than a picogram of rhodopsin. Human rhodopsin has its peak absorption around 500 nm (extinction coefficient 40 500 M^{-1} cm^{-1}), a broad and flat absorption band that extends into the near ultraviolet, and a steep roll off to minimal extinction by 620 nm.[13] Photon absorption anywhere in this band can activate rhodopsin.[14] During activation the 11cRet chromophore isomerizes to its all-trans isomer in the initial and sole photochemical conformational step in activation that results in Bathorhodopsin formation within 200 femtoseconds.[15] Following this, rhodopsin undergoes a series of thermally triggered conformational transitions with unique absorption band characteristics and progressively longer lifetimes.[16]

We are predominantly interested in the Metarhodopsin-I (Meta-I)→Metarhodopsin-II (Meta-II) state transition which occurs on a millisecond time scale. In this conformational transition rhodopsin enters into a biochemical state where it binds and activates the G-protein, transducin, which then communicates rhodopsin activation to the biochemical and physiological transduction cascade in the rod photoreceptor. Rhodopsin signaling in this cascade generates the first step in vision. During Meta-II formation the Schiff base deprotonates to an internal residue and two protons are taken up into the cytoplasmic face of the protein. This results in a global conformational change in rhodopsin that involves a large increase in molecular volume.[17–19] The biochemically measured proton exchange reactions lend support that the electrophysiological signals of rhodopsin activation could be measuring the same conformational transitions in rhodopsin on the millisecond time scale.[20]

Absorption spectrophotometry and Fourier transform infared spectroscopy have been applied to expressed normal and mutant rhodopsins in tissue culture. Difference spectra between the ground state and Meta-II have been reported using these methods.[21–25] The temporal appearance and properties of these rhodopsin intermediates could be studied by time-resolved absorption and infared spectroscopy but this would require milligram levels of protein.[26] These quantities of visual pigment are not readily generated in a mammalian cell expression system for the normal opsin, let alone opsin mutants which may not express as well.[27] Only electron spin resonance spectroscopy, with covalently attached spin probes at engineered cysteine residues, has been able to begin to address the temporal resolution of conformational states in accessible environments of otherwise normal rhodopsin expressed in cultured cells. Yet, exploration of the effects of site-specific mutations in the opsin protein on the temporal process of activation is an area of very important research. For example, it is still not clear how conformational transitions in the chromophore environment are communicated to the cytoplasmic face of rhodopsin where protons enter and transducin binds.[28–30] We were therefore interested in other assays that would have the sensitivity to explore the conformational activation of mutant rhodopsins that could be expressed in smaller amounts.

Rod rhodopsin is uniformly oriented in both disk and plasma membranes. Within picoseconds after photon absorption there is a charge separation in the 11cRet binding pocket that helps to store photon energy.[16] Due to rhodopsin orientation this charge separation can be recorded across the membrane as a voltage known as the R_1 phase of the early receptor potential (ERP).[31] After this early charge separation there is no net electrical activity in rhodopsin until the time frame of Meta-II formation. During Meta-II, and temporally correlated with known proton exchange reactions, is a much larger and vectorially opposite electronic transition known as the R_2 phase of the ERP. This charge flow occurs from about 100 μs to 5 ms, and thus overlaps the critical formation of Meta-II from Meta-I.[32–34] Studies of R_2 constitute a physiological assay of time-resolved electrically active conformation changes in rhodopsin (Sullivan, work in progress). The R_2 phase of the ERP, or its companion the ERC, has been used to: (1) measure the amount of rhodopsin in photoreceptors,[35] (2) follow the kinetics of the thermal transitions of rhodopsin,[8,36,37] and (3) assay the photosensitivity of rod and cone visual pigments.[38] Each of the known spectral states that can be thermally trapped appears to have its own ERP state signature.[39–41] Since these signals can be recorded at a single photoreceptor cell level, the ERC/ERP is potentially a very informative time-resolved assay of visual pigment conformation changes. The ERC/ERP signal belongs to a family of conformation-dependent currents, for example, like the gating currents of ionic channels.[42] In expressed mutant pigments ERC/ERP studies could yield important information about the role particular amino acids play in both the normal biophysical and biochemical activation process and in abberant activation processes of mutant human opsin pigments that promote hereditary retinal degeneration.

C. Design needs

Previous studies of the ERC/ERP mostly used xenon flash systems,[35,37,38] although shutter-controlled tungsten lamp[8] or laser[31,34,43,44] delivery systems were sometimes used. In some studies xenon flash intensities were insufficient at the specimen plane to allow use of interference filters to stimulate the ERC/ERP.[35,37] In this case equivalent flash intensities in the bandwidth of interest were calculated from the composition of the white flash delivered. Electromechanical shutter-controlled systems[8] were only capable of relatively long duration flashes of a few milliseconds. Makino[38] delivered high intensity monochromatic flashes, several hundred microseconds in duration, by mounting the xenon flash tube in the immediate environment of the electrophysiological recording apparatus to maximize throughput. However, this resulted in a large electromagnetic flash artifact which polluted ERC data acquisition and necessitated careful subtraction. Use of nitrogen-stimulated dye lasers[44] was highly efficient to deliver intense monochromatic flashes into diverse geometries, but the need to handle dyes can be cumbersome and the expense of such a system is likely to be prohibitive to many laboratories.

For these reasons a xenon flash delivery system was designed and constructed to generate microbeams of light in the optical specimen plane of an inverted microscope used for single-cell electrophysiological recording. There were several significant design constraints. First, the flash needed

to be of sufficient intensity in order to stimulate oriented rhodopsin pigments having a photosensitivity of approximately 10^{-8} μm^2. Thus, the light intensity needed to be at least 10^8 photons/μm^2 to have multiple photons per rhodopsin molecule. Second, the flashes needed to be monochromatic or at least band limited. Third, the flash duration needed to be less than 50 μs such that photon delivery would not overlap with the temporal conversion of Meta-I to Meta-II in a way that could result in second photon absorptions and photoreversal to prior spectral states or rhodopsin.[45–49] Thus the flash needed to be an impulse (Dirac) stimulus relative to Meta-II formation in order to record rhodopsin ERC charge motions associated with the biochemical phase of activation. Fourth, the flashes needed to be optically coupled to the specimen plane such that there would be no electromagnetic interference with the ERC data acquisition hardware. Fifth, the flash intensity needed to be measured with each impulse such that the true stimulus presented would always be absolutely known to compensate for photon flux statistics and xenon flash tube jitter. Sixth, the flash delivery plane should be parafocal with the specimen image plane to avoid complex adjustments of the flash delivery plane once a single cell is microscopically chosen and imaged for study. These design constraints presented significant electro-optical engineering challenges.

To summarize, desired factors in a bright flash microbeam delivery system were: (1) microscope coupling to form a microbeam over a single cell in the recording chamber, (2) short flash duration on the order of 10 μs so that the Meta-I formation could also be examined electrically, (3) monochromatic flashes at very high intensity (goal: 10^9 photons/μm^2), (4) no electromagnetic radiative interference of the flash pulse into the electrophysiological recording hardware, (5) low cost, (6) the measurement of delivered flash energies on an impulse-by-impulse basis, and (7) suitable tools for calibration and for hardware/software enhancements.

All design goals were achieved. Microbeam monochromatic flash intensities of 10^8-10^9 photons/μm^2 were obtained in the prototype (Flash 1). Flash durations were less than 20 μs. Flashes were delivered to the microscope on a fiber optic which prevented electromagnetic pulse noise delivery to the recording apparatus. Finally, an optical delivery system was designed to measure the absolute intensity of each flash using a calibrated photodiode. The apparatus is capable of eliciting ERC currents from single cells expressing less than one picogram of opsin. Moreso, submillisecond resolution of ERC charge motions was achieved. The utility of the device is immediately extendable to all types of photoreceptors or cells containing photolabile pigments. In addition the device might be used for cells loaded with caged compounds to liberate physiologically active agents by photolysis.

II. MATERIALS AND METHODS

A. Flash apparatus

All electro-optical components were enclosed in an aluminum box with a second internal Faraday cage surrounding the xenon flash tube and its associated electronics. The xenon can flash tube (7 J) with a 1 mm electrode gap, its trigger module, surge diode, flash capacitor (oil, 40 μF, 1000 V), and power supply were all obtained from EG&G (Salem, MA). The flash leaving the internal box shield was collimated using a doublet of fused silica lenses (OptiQuip Inc., Highland Mills, NY). This doublet results in a combination focal length (f.l.) of approximately 25 mm with the lenses touching at their optical centers. Twelve three-cavity bandpass interference filters, blocked 10^{-4} out of passband (Omega, Brattleboro, VT) were mounted in a panel-controllable wheel and aligned in the collimated white flash beam. The monochromatic flash was then imaged using a second doublet of identical fused silica lenses onto the face of a 1 mm core fused silica fiber optic [0.42 numerical aperture (NA)] (Technical Video Ltd., Woods Hole, MA). The fiber was aligned with a three-dimensional chuck (Oriel Corp., Stratford, CT). All optics were mounted in holders (Melles Griot, Irvine, CA) and positioned using linear microrails (Newport Corp, Irvine, CA).

Panel (binary coded decimal) switches and digital-to-analog circuitry were used to modulate a dc control voltage to the flash power supply in order to regulate its voltage output and thus the electrical energy stored in the flash capacitor. The flash capacitor voltage was measured, analog circuitry converted volts to joules ($E=CV^2/2$), and the results were displayed on a panel-mounted liquid crystal device. The flash was triggered either manually by a panel mounted pushbutton, by an external TTL pulse from a computer, or by a panel-programmed internal oscillator with a count-to-N-and-stop function. A light-emitting diode display counted flashes. All circuit boards except the flash power supply were designed and fabricated to instrument specification.

B. Microscope elements

A modified Nikon Diaphot inverted microscope was used for viewing cells during electrophysiological experiments. An attached CCD camera (Sanyo) permitted remote viewing of electrode placement onto cells using transmitted infared light that does not bleach the visual pigment. The microscope was housed in a continuous aluminum Faraday cage that was internally coated with black felt. The lamphouse of the microscope was placed outside and on top of the Faraday cage to exclude visible light from the recording environment. The light from the source passed through an infrared (>830 nm) long pass filter before entering the cage and was communicated to the long working distance Nomarski-differential interference contrast (DIC) condenser using relay lenses. Using white light the microscope was adjusted to achieve Koehler illumination to maximize image contrast;[50] reasonable contrast in the infared was also achieved.

For an objective lens to efficiently condense light energy emmanating from the fiber optic into a microbeam, the specimen plane of the microscope and the fiber-optic face plane needed to be conjugate field planes (Inoue, 1986). The specimen plane is a conjugate field plane with the intermediate

image plane of the microscope which lies 150 mm below the shoulder of the objective. This point was not readily accessible in the Nikon Diaphot microscope, so an alternative delivery system was designed. The fiber optic was routed through the Faraday cage to the microscope epifluorescence port. A fiber-optic adapter (Model No. DX-4 body without lenses; Technical Video Ltd., Woods Hole, MA) was used to connect and align the fiber optic with respect to the optical axis of the microscope at the level of the turret. The fiber is then constantly positioned with respect to the objective to deliver a focused microbeam regardless of the movement of the optical turret to bring a cell into focus. A custom dichroic mirror was designed (Omega, Brattleboro, VT) both to reflect the near ultraviolet and visible light energy (320–650 nm) exiting the fiber into the rear objective aperture and to transmit above 675 nm for infrared CCD viewing of the specimen plane. The dichroic was mounted at 45° in a dedicated Nikon epifluorescence filter cube. The entrance port of the cube was modified so that a custom lens holder could be inserted. A doublet of a planoconvex lens (18 mm f.l.) and a positive meniscus lens (23 mm f.l.) (Edmund Scientific, Barrington, NJ) were used to collimate the output of the fiber optic prior to the 45° dichroic mirror plane. The collimated beam width was about 6 mm diameter and reasonable collimation length was calculated and confirmed to be about 60 mm. The collimated flash beam reflected off the dichroic, passed through the infinity correction lens intrinsic to the microscope turret, and was presented to the rear aperture of the objective lens. The presentation of collimated light to the rear aperture of the objective lens insured that the specimen and fiber were in conjugate field planes and allowed the objective to condense much of the flash energy into a microbeam spot. In this configuration the maximum spot size in the specimen plane is inversely proportional to the ratio of the objective f.l. to the doublet f.l.:

$$\text{Spot diameter} = (\text{Fiber Core diameter})(\text{Objective f.l.}/\text{Doublet f.l.}). \quad (1)$$

C. Optical alignment

To align flash delivery optics the internal 0.05 μF capacitor in the flash power supply was used to delivery a low intensity flash train since the external flash capacitor (40 μF) cannot tolerate the rapid frequency pulses (e.g., 50–100 Hz) needed to generate an effectively continuous beam to the powermeter. First, the fiber output face was stably positioned and aligned directly against the window of the calibrated photodiode (Model 400; 3M Photodyne Corp, Camarillo, CA) of a μW/μJ meter (66XLA; 3M Photodyne) functioning in μW mode. In the flash box the xenon tube, the fused silica doublets and eventually the fiber input face were manipulated until maximum optical power delivery (throughput) to the photodiode was determined. Minor variations in position of all optical pieces were then made to insure that maximum global throughput had been achieved.

The output end of the fiber was inserted into its chuck in the turret of the epifluorescence port and a cross hair target was placed in the specimen plane. Without an objective lens the fiber was moved along its axis until the focused image of the flash was seen on the cross hairs due to the action of the lens doublet in the cube and the infinity correction lens in the turret. The cross axis adjustment screws on the adapter chuck were used to move the focused flash circle until it was centered on the cross hairs. The 40× objective was then swung into place and the cross hairs moved to align with the microbeam spot that was imaged visually with a magnifying lens train aligned above the specimen plane. The objective was removed again and the large spot found to be centered on the target. Remaining offsets were corrected by small iterative adjustments until there was no shift of the spot with respect to the target crosshairs once the objective (condenser) was swung into place.

D. Light measurements

To measure each flash during electrophysiological recordings, additional optics were required. The long working distance Nomarski/DIC condenser (Nikon Diaphot) was designed to image the lamp house diaphragm aperture into the specimen plane, which are both field planes.[50] With the lamp house moved vertically with the assistance of relay lenses, there was sufficient space to use the Nomarski condenser in reverse fashion to generate a magnified image of the microbeam spot in the specimen plane into the original but orthogonally offset plane of the lamphouse condenser diaphragm aperture, in effect acting like an additional microscope. A photodiode placed at this plane was used to measure the energy in each flash. To accomplish this a second dichroic mirror was manufactured with matched optical properties to that used in the epifluorescence cube. This 45° dichroic mirror was mounted on a remotely controlled and mechanically quiet drive mechanism situated at 90° to the optical axis and mounted above the condenser and below the relay lenses. The mirror was inserted or removed from the optical path as needed. The mirror/photodiode holder was constructed with an attachment for aligning and focusing of the magnified microbeam flash to fill the sensor surface of the calibrated photodiode for most efficient recording (μJ) by the meter.

The optical transmission properties between the specimen plane and the photodiode were characterized in two stages. First, the condenser of the microscope was aligned for Koehler illumination and the DIC condenser iris position marked. Continuous monochromatic spectral fluxes generated with a monochromator were delivered to the specimen plane through the 1 mm core fused silica fiber optic. Light input to the monochromator originated from a 150 W quartz tungsten halogen lamp mounted in a housing with a rear reflector assembly and a fused silica condenser (Model Q, Oriel Corp., Stratford, CT). The condenser collimated the output of the lamp and the lamp filament was imaged onto the input slit of the monochromator using an additional 150 mm f.l. lens operating at F/No. 4.5. The 0.2 m concave holographic grating monochromator (1200 g/mm) (F/No. 4.2) (Model 275; Schoeffel-McPherson, Acton, MA) was used to generate monochromatic light with its exit slits set for 10 nm dispersion. The output cone of the monochromator was col-

limated using an additional 150 mm f.l. length double convex lens operating at F/No. 4.5 and was imaged into the fiber optic using an 38 mm f.l. double convex lens operating at F/No. 1. The fiber delivered light to the microscope through the epiflourescence port and microbeams were generated in the specimen plane. The monochromatic light intensity of the microbeam was quantified across the spectral band using the calibrated photodiode (μW mode) aligned immediately above the selected objective lens. Next, the microbeam spot in the specimen plane was imaged onto the photodiode using the described optical train but with the DIC condenser iris diaphragm fully open to maximize throughput to the photodiode. The ratio of monochromatic light power delivered and measured at the photodiode plane over light power delivered to the specimen plane constituted the percent transmission at each wavelength.

During routine calibration and alignment of the fiber optic in the epifluorescent port holder, the 400S photodiode was mounted on a vertical optical rail attached to the microscope stage and its window placed directly on top of the objective. Under this configuration the photoactive surface is not overfilled (vignetted) and the diode does not saturate with the flash such that absolute energy measurements are obtainable.

Measurements of flash duration were made with a MRD721 PIN photodiode in parallel with a 50 Ω resistor and observed on a triggered analog storage oscilloscope. The waveform was inverted for observation. Between the flashlamp and the photodiode a 2.0 log neutral density attenuation filter was interposed to avoid PIN diode saturation during measurements of flash duration. Waveforms were traced off of the scope.

E. Measurement of microbeam spot sizes

The spot size in the specimen plane is expected to be a point spread function (PSF) of energy due to the diffraction properties of the objective lens. Without complete microscope objective specifications it was not possible to calculate its explicit appearance. Instead the PSF was measured in one dimension using a precision 50 μm optical slit (Model No. N38,559, Edmund Scientific, Barrington, NJ). The slit was mounted with its long axis orthogonal to the motion axis of a small unidimensional linear drive with a fine screw (80 threads per inch) (Model No. MM-3; Daedal, Harrison City, PA). The 400S photodiode was placed immediately above the slit and aligned with the optical axis. Monochromator generated light of 500 nm was delivered to the epifluorescent port using the 2 m fiber optic. The fine screw on the linear manipulator was turned through a measured number of degrees causing a linear movement of the slit occurred across the optical axis in a single dimension. The light intensity (μW) was measured as the slit scanned the microbeam spot. The throughput intensities were normalized to peak throughput to generate a single axis view of the complex three-dimensional PSF. The full width half maximum (FWHM) of the Gaussian-shaped distribution was used as the spot size diameter. Spot size diameters were corrected slit width as follows:[51]

$$(\text{Measured PSF})^2(\text{FWHM}) = (\text{Slit Width})^2 + (\text{True Image Width})^2(\text{FWHM}). \quad (2)$$

F. Cell growth and rhodopsin regeneration

HEK293S cells stably transformed to express WT human rod opsin were grown on poly-L-lysine coated glass coverslips in DMEM/F12 medium (Life Technologies, Gaithersburg, MD) with 10% calf serum and antibiotics at 37 °C and 5% CO_2.[21] Each of these cells expresses about 10^7 opsins with most of the opsin partitioned to the plasma membrane. After several days of growth coverslips were placed in the dark in electrophysiological recording buffer and 25–50 μM 11cRet was added. After pigment regeneration over about 30 min, coverslip fragments were transferred to identical recording medium without 11cRet in the microscope chamber. After rhodopsin regeneration and during transfer of the coverslip fragments to the recording chamber, dim red darkroom light was used which does not bleach rod visual pigment (Kodak GBX-2 Safelight Filter). Once in the recording chamber infared light (>830 nm) was used for cell imaging.

G. Electrophysiological recording

Gigaohm seal patch clamp recording was according to Hamill *et al.*[12] Micropipetes (salt bridges) were fabricated from borosilicate glasses using two stage pulls (Model 730 Needle/Pipete Puller, Kopf Ind, Tujunga, CA). They were coated with black Syllgard (Model No. 170A&B; Dow Chemical, Midland, MI) to decrease capacitance-coupled current noise and prevent light from the flash from spreading up the microelectrode waveguide to the Ag/AgCl electrode. The recording electrode immersed in the pipete was a Ag/AgCl pellet, and the bath electrode was a Ag/AgCl electrocoated wire. Micropipetes were filled with (in mM): 10 KCl, 120 KF, 1.0 $CaCl_2$, 2.0 $MgCl_2$, 11.0 EGTA-KOH (pH 7.2), and 10 HEPES-KOH (pH 7.2). Bath solution was (in mM): 140 NaCl, 5.4 KCl, 1.8 $CaCl_2$, 1.0 $MgCl_2$, 10 HEPES-NaOH (pH 7.2). Recording pipetes were backfilled, sealed in a polycarbonate holder, and inserted into the Teflon junction of the patch clamp headstage (CV-4, Axon Ind., Foster City, CA). The headstage was mounted on a combined three-dimensional coarse/ultrafine hydraulic micromanipulator. The headstage was connected to the patch clamp amplifier (Axopatch 1C, Axon Ind).

The infared sensitive CCD camera and a television provided visual feedback for pipete placement on cells using 830 nm light which is beyond human visual spectral range. Reasonable DIC contrast was obtained even at >830 nm transmitted light despite the fact that the objectives are optimized for 535 nm. The TV image of the electrode approaching the cell surface was integrated by the user with the tonal output of an audio impedence circuit in the patch clamp amplifier which measured pipete resistance. This assisted with precise recognition of when the pipete first touched the cell. Just at this point the oscilloscope traces showing an increase in pipete resistance relative to the bath ground during test voltage stimuli. Slight suction ($\approx$10 cm H_2O) was then used

to generate gigaohm seals. The gigaohm seal both decreases the background shunt noise during recording and is mechanically stable such that the underlying patch of membrane can be broken to give a low resistance access impedence into the whole cell while maintaining a very high resistance shunt pathway around the electrode.

After forming the seal the pipette/seal capacitance was compensated with the amplifier by minimizing the capacitative current transient to a train of voltage steps. The patch of membrane underlying the pipete was broken with a pulse of suction to enter the whole-cell recording mode (WCR). A large increase in capacitative current (whole-cell) to the voltage steps indicated entrance into the WCR. Whole-cell capacitance and the series resistance of the electrode were then compensated electronically with the amplifier in order to optimize recording of ERC kinetics. Slow ramp voltage clamps were then delivered under WCR using pCLAMP 5.51 (CLAMPEX) (Axon Ind.) and an interface card (100 kHz, Scientific Solutions, Akron, OH) which controlled analog/digital conversion, digital-to-analog outputs for voltage control of the patch clamp, and digital signals for device and oscilloscope triggering. Ramp voltage clamp allowed identification of the intrinsic conductances of HEK293 cells, the leakiness of the cell which will shunt the ERC recordings, and the zero current potential at which whole-cell current noise was expected to be minimal. The holding potential was then set near this potential. High intensity flashes were then delivered to the cell using the microbeam apparatus and the ERC recorded. Data were recorded onto the computer hard drive using CLAMPEX or AXOTAPE (Axon Ind., Foster City, CA) and concurrently in parallel onto VCR tape using a digital data recorder interface (Model VR-10; Instrutech, Elmont, NY) and a VCR recorder (Panasonic 1240). An 8-pole Bessel filter was used between the output of the patch clamp amplifier and the analog/digital hardware interface (Model LPF902B, Frequency Devices, Haverford, MA). The internal 4-pole Bessel filter of the patch clamp was set at 10 kHz (-3 dB down) and the 8-pole Bessel set at 2–5 kHz.

III. RESULTS

A. Bright flash microbeam optical design

Xenon was acceptable as an excitation source because of its low ionization energy[52] and its broad spectral band with peaks over the near-UV and visible.[53–55] In addition a wide selection of relatively inexpensive flash lamps and control electronics were commercially available as well as extensive research on their properties.[56–61]

To avoid electrophysiological flash artifacts due to electromagnetic or mechanical noise, the flash power supply, flash tube, flash capacitor, triggering elements, and associated electronics were remotely housed in a doubly shielded aluminum box away from the Faraday recording cage. Fiber optic transfer to the recording environment required an element with high efficiency transfer across the desired spectral band. In addition the fiber was chosen to maximize energy throughput and delivery to the specimen plane given the geometric optical constraints at the input and output ends of the fiber. Previous work helped to establish fiber core size limits

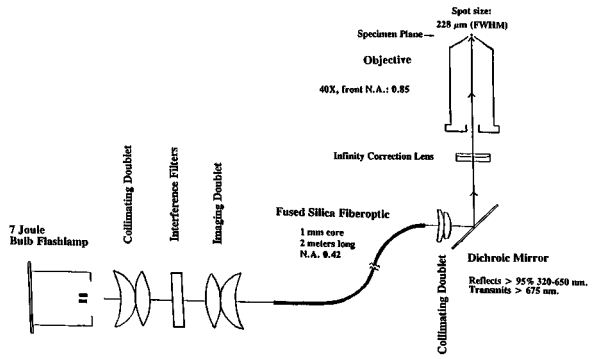

FIG. 1. Bright flash microbeam design. A schematic of the flash collection and delivery system to the specimen plane is shown with the 40× Fluor lens (NA = 0.85).

which could be used to efficiently couple into the rear aperture of a high NA microscope objective.[62,63] A medium-core (1 mm) fused silica fiber optic (0.42 NA, 2 m long) was selected to deliver the light from the flash box to the epiflourescence port of the inverted microscope which provided the coupling input to the objective to generate microbeams. The dichroic mirror for the epiflourescence apparatus permitted efficient energy delivery from 320 through 650 nm into the objective and forward transmission of near IR (830 nm) for CCD camera viewing of the cell and pipete placement for WCR. To couple the light cone from the fiber through the objective into the specimen plane a four lens optical system was designed including the two lenses at the output of the fiber, the intrinsic infinity correction lens of the microscope, and the objective lens. A system schematic is shown in Fig. 1.

Attention was then directed toward a high geometric effiency, high intensity monochromatic flash coupling to the input end of the fiber. Four fused silica lenses were selected to constitute the optical coupling train from the flash lamp into the fiber. The flash from a 1 mm short-arc 7 J bulb-type xenon flash lamp was collimated by a fused silica doublet designed to collect at approximately 0.95 steradians (full sphere collection = 12.56 steradians). Three-cavity, high-transmission bandpass interference filters (10 and 70 nm at FWHM), positioned in the region of collimation, generated band-limited flashes over the near-UV and visible spectrum. A second identical fused silica doublet imaged the collimated monochromatic flash into the 1-mm-core fused silica fiber optic. From the flash tube specifications an electrical-to-spectral energy conversion a radiation transfer calculation indicated that approximately 10^9 photons/μm^2 would arrive in the microbeam spot. The fiber input end of the flash apparatus contained homemade electronics for generating the flash trigger pulses, counting the flash pulses, controlling the filter wheel, measuring, displaying, and modulating the voltage or energy stored on the flash capacitor, manual and computer interfaces to control the filter wheel position, and power generation.

B. Microbeam spot size

The charges moving per rhodopsin activation are linearly related to the amount of pigment activated.[35,41] In order

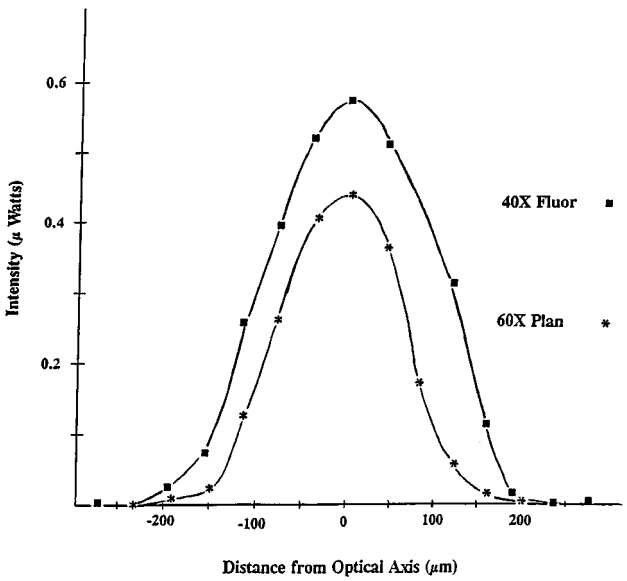

FIG. 2. Microbeam shape and diameter. The microbeam was focused onto the specimen plane and scanned in one dimension with a precision 50 μm slit mounted on a microminiature manipulator. The input to the fiber optic was 500 nm light from a single McPherson 275 monochromator. Light transmitted through the slit plane was measured using the calibrated photodiode placed just above the slit. The peak of the point spread function was commensurate with the microbeam being centered on the optical axis. The full width half maximum (FWHM) diameter of the microbeam spot (true image width) is 228 μm (40× Fluor Achromat, NA=0.85, f.l.=4.16 mm) or 155 μm (60x Plan Achromat, NA=0.85, f.l.=2.6 mm).

to activate as much rhodopsin as possible, the flash energy needed to be coupled into a small a geometric area over a very brief flash duration. An implicit requirement was that the spot size of the flash in the microscope specimen plane needed to be minimized toward the limit of the geometry of the HEK293 cells ($\sim$16 μm diameter) and the calculated effective collecting area. This required a short-arc lamp, a geometrically efficient flash-to-fiber and fiber-to-specimen coupling system, and a fiber core size maximizing throughput but not exceeding the geometric limits of the microscope objective acting as a condenser. The collection and delivery of a large percentage of the available monochromatic flash energy into the specimen plane was due to a geometrically efficient optical delivery train in which the flash tube arc gap and the fiber-optic core diameter were matched with an efficient optical delivery system.

The energy distribution in the microbeam spot was expected to be a three-dimensional Gaussian PSF. In order to determine the shape of the light intensity distribution in the specimen plane and measure the spot size, the microbeam spot was scanned with a 50 μm precision slit and the light intensity (500 nm) throughput measured with a photodiode. With a selected 40× near-UV-visible transmitting objective (front NA=0.85) the imaged spot in the specimen plane was determined to be 228 μm at FWHM for the Gaussian-shaped PSF (Fig. 2). With the 60× objective (front NA=0.85) a 155 μm spot diameter (FWHM) was found. The decrease in spot size with increasing objective power is reflective of the decreasing rear numerical aperture with decreasing objective f.l. The measured FWHM spot diameters were consistent with computed estimates of the maximum spot diameter using Eq. (1) given that the fiber has a 1 mm core and the doublet has a f.l. of approximately 10 mm (416 and 263 μm for 40× and 60× lenses, respectively).

Since the average diameter of single HEK293 cells is about 16 μm, the spot size will always be at least ten times the cell size and thus will be uniformly presented. Larger spot sizes will also facilitate uniform stimulation of fused HEK293 cells with diameters as high as 75–100 μm. As the PSF is aligned with the optical axis of the microscope, the most intense and uniform aspect of the spot will overly the cell which is also positioned on the optical axis. No gradients of light are expected in a single cell and all the pigment or chromophore is expected to be exposed to the same flash intensity. The percent flash energy in the FWHM area is 84.4% (40× Fluor) and 80.4% (60× plan).

C. Flash microbeam intensities

The microbeam light intensity (photons/μm^2) needed to be greater than 10^8 across the near UV through visible (350–650 nm). This value was chosen based upon the photosensitivity of rhodopsin of approximately 10^{-8} μm^2.[64] The photosensitivity is the product of the quantum efficiency ($\approx$0.67) and the molecular cross section of the rhodopsin pigment. The criterion level of flash intensity was necessary to insure a high probability that each rhodopsin molecule in a single cell can absorb at least one photon per flash. With the 7 J flash lamp monochromatic microbeam intensities were $1.5-3\times10^8$ photons/μm^2 across the near-UV-visible spectrum using 10 nm FWHM filters and $4-6\times10^8$ photons/μm^2 using 70 nm FWHM filters [Fig. 3(A)]. These measurements were made with the DIC elements of the microscope in place between the dichroic mirror and the objective. When these are removed to decrease optical pathlength, flash intensities increase 24–37% for the 40× objective and 43–62% for the 60× objective depending upon the wavelength. Based upon the level of 9×10^6 rhodopsins/HEK293 cell, and assuming an exponential distribution function for the fraction of rhodopsin molecules absorbing one photon per flash,[38] current intensities are sufficient to achieve 84% (10 nm FWHM) or 99% (70 nm FWHM) absorptions with a single maximum intensity 7 J flash.

However, a single flash of microsecond duration can bleach a maximum of only 50% of the available pigment because of photoregeneration from short-lived intermediate states.[45,46] That is, when the flash intensities are sufficiently high and the duration and spectral characteristics of the flash overlap with absorbing intermediate states, a second photon can be absorbed by an activated molecule promoting a photoregeneration of the ground state. Thus, an ERC signal can only be obtained from a maximum of 50% of the available ground state rhodopsin present prior to a flash. Microbeam flash intensities with this instrument are sufficient to bleach the residual amount of rhodopsin remaining after each flash. Therefore, to extinguish the ERC signal of a given cell containing regenerated rhodopsin a series of high intensity flashes must be given. The decay of the signal with flash number follows an exponential distribution[8,38] and the number of flashes required to extinguish the pigment depends

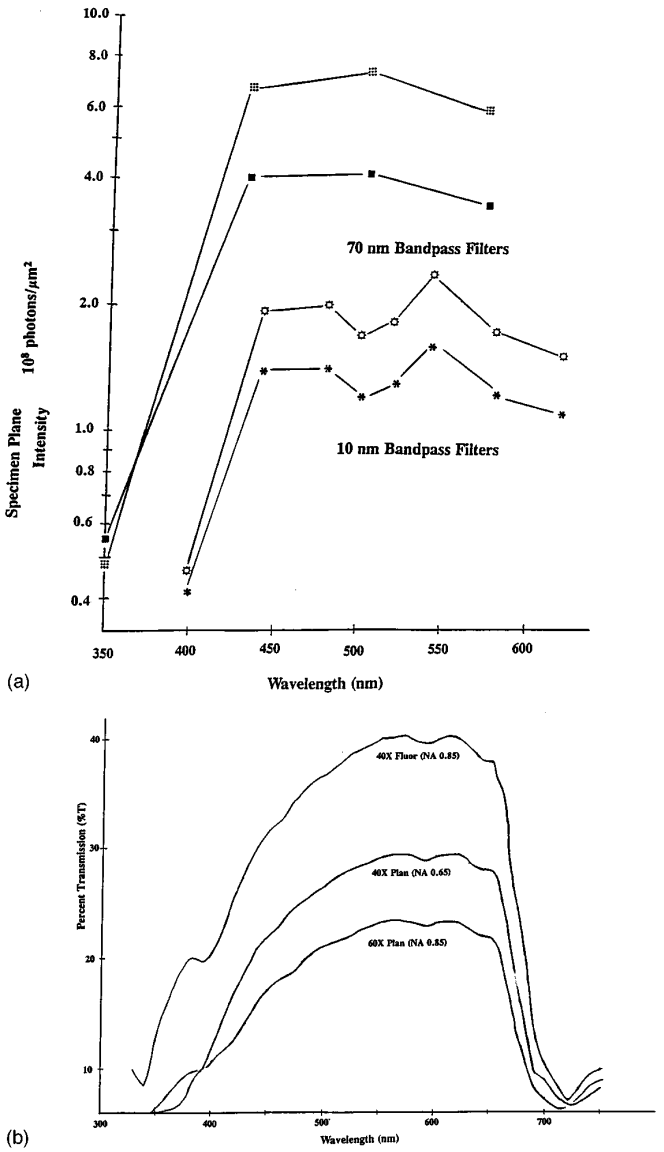

FIG. 3. Microbeam intensities in the specimen plane. (A) Flash intensities in μJ were measured in the specimen plane using a calibrated photodiode joulemeter positioned immediately above the objective lens on the optical axis. μJ were converted to absolute photons/μm^2 using energy constants at the wavelength peak of the interference filter and then divided by the microbeam spot size area (at FWHM) obtained from point spread function analysis. The results were obtained with the DIC optical elements in place below the objective (without these intensities are 24–37% greater for the 40× lens and 43–62% greater for the 60× lens. Filters in the flash microbeam box are three-cavity elements and either 10 or 70 nm at FWHM. Figure is labeled as: * and ■ (40× Fluor Objective, NA=0.85), ☼ and ⁞⁞⁞ (60× Plan Objective, NA=0.85). (B) The transmission spectrum of the delivery system between the fiber output face and the specimen plane are shown with the DIC elements in place for three objectives.

upon the amount of remaining pigment in a cell and the flash intensity used for bleaching.

To characterize flash intensity losses in the microscope optical delivery system, the spectral transmission efficiency from the fiber output to the specimen plane was determined with the DIC attachments in place [Fig. 3(B)]. The raw spectral output of the fiber was first measured using the calibrated photodiode and a continuous monochromator-generated input stimuli. Then the fiber was replaced and aligned in the epiflourescence apparatus and the light intensity (μW) measured in the specimen plane above the objective. Spectral transmission from the fiber to the specimen plane varied considerably with different objectives. The best objective tested was the 40× Flour lens (0.85 NA) achieving nearly 40% transmission in the visible with a clear near-UV peak (about 20%). Relative to a low-cost 40× objective (0.65 NA) the transmission is considerably greater. This results from two factors. First, the back NA of an objective is given by

$$\text{Back NA} = (\text{Front NA})/(\text{Objective Power}). \quad (3)$$

The back NA is thus greater for the 0.85 NA 40× lens than the 0.65 NA 40× lens because of greater collection by the 0.85 NA lens. Second, the physical pupils of the two objectives are slightly different, permitting greater throughput for the 40× Flour lens when presented with a collimated beam at its rear aperture. The different transmissions of the 40× and 60× 0.85 NA lenses relate to the decreased back NA for the 60× lens thus decreasing its throughput. In the prototype optical design throughput is proportional to the (back NA).[2] Without the DIC system in place the plateau of the transmission spectrum increases to 55%, 44%, and 35% for the 40 × Fluor (NA 0.85), 40× (NA 0.65), and 60× Plan (NA 0.85) lenses, respectively.

Using an optical delivery system which collimates the light leaving the fiber, microbeam intensities are most affected by the optical pathlength in the system and the optical and transmission characteristics of the objectives used. Alternative optical delivery systems that recondense the light leaving the fiber are likely to enhance throughput above these values (Sullivan, work in progress).

D. Flash duration at various stimulus strengths

The major conformational transition supporting biochemical activation of rhodopsin is the Meta-I to Meta-II transition which has a rate of formation of a few milliseconds at physiological temperatures. The reaction from Lumirhodopsin to Meta-I has a rate of formation of a several microseconds at physiological temperatures. The flash duration needed to be as short as possible, certainly to provide an (Dirac) impulse stimulus to measure the rhodopsin ERC charge redistribution concurrent with spectral Meta-II formation, but also to attempt to record the Meta-I formation using subphysiological temperatures. The design target for pulse duration was set at 50 μs. The type of lamp chosen allowed for brief flashes. The design of the electronic circuit and the wire connections from the flash capacitor to the lamp were kept short to minimize inductance and pulse duration.

Using a fast photodiode to record the rise time and pulse duration the flash was found to be only 14 μs at FWHM using a full 7 J charge on the capacitor (Fig. 4). Flash duration decreases with lower energy discharges from the capacitor. The rise time of the light output is under 5 μs. Thus, both microbeam flash intensity and flash duration matched design goals.

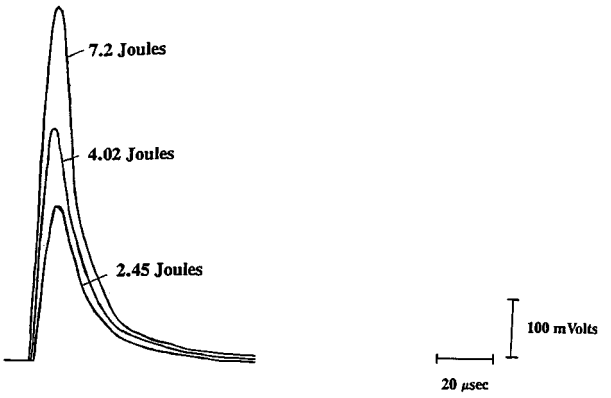

FIG. 4. Flash duration at various stimulus strengths. The 7 J bulb-type flash lamp pulse duration was measured with a MRD721 PIN photodiode in parallel with a 50 Ω resistor and observed on a triggered oscilloscope. The waveform was inverted for observation. A 2.0 neutral density attenuating filter was interposed between the flash lamp and the photodiode to avoid PIN diode saturation and obtain accurate measurements of the light pulse output.

E. Flash-by-flash measurement of intensity

The system was designed with the capacity to measure the monochromatic microbeam flash intensities in absolute photons/μm^2 obtained on a flash-by-flash basis. This facility allows the experimenter to compensate for flash intensity variability due to, among other parameters, photon flux statistics and xenon flashtube ''jitter.'' By mounting the calibrated photodiode above the long working distance DIC condenser of the microscope at a point equivalent to the lamphouse condenser field diaphragm plane, the specimen plane and the photodiode surface become conjugate field planes [Fig. 5(A)]. Provided that the photodiode is not overfilled and the transmission spectrum of the optical train between these planes is known, absolute photons/μm^2 in the specimen plane can be calculated using the calibration curve of the photodiode and the measured FWHM microbeam spot diameter for a given objective. The transmission spectra from the microscope specimen plane through the long working distance condenser, the dichroic mirror and other losses along the path to the calibrated photodiode was measured [Fig. 5(B)]. Transmission between the specimen plane to the photodiode varies from about 25 to 35% for 0.85 NA lenses to between 40 and 55% for 0.65 NA lenses. This is a direct consequence of the front NA of the lenses and the more compact cone of light delivered with the 0.65 NA objective lens that can be more efficiently collected by the long working distance condenser (0.52 NA).

The voltage output of the 66XLA joulemeter is linearly proportional to μJ. The integrating circuit in the 66XLA amplifier is zeroed just prior to the flash using a correlated digital pulse. The photodiode/joulemeter integrates the charge flow resulting from the photon absorption resulting in a voltage step function at the analog output of the meter. The amplitude of the voltage step is linearly proportional to the measured energy. The μJ measured with each flash can then be used to calculate absolute photons/μm^2 in the specimen plane microbeam spot at a given wavelength. This is done by multiplying the voltage output by both the photodiode cali-

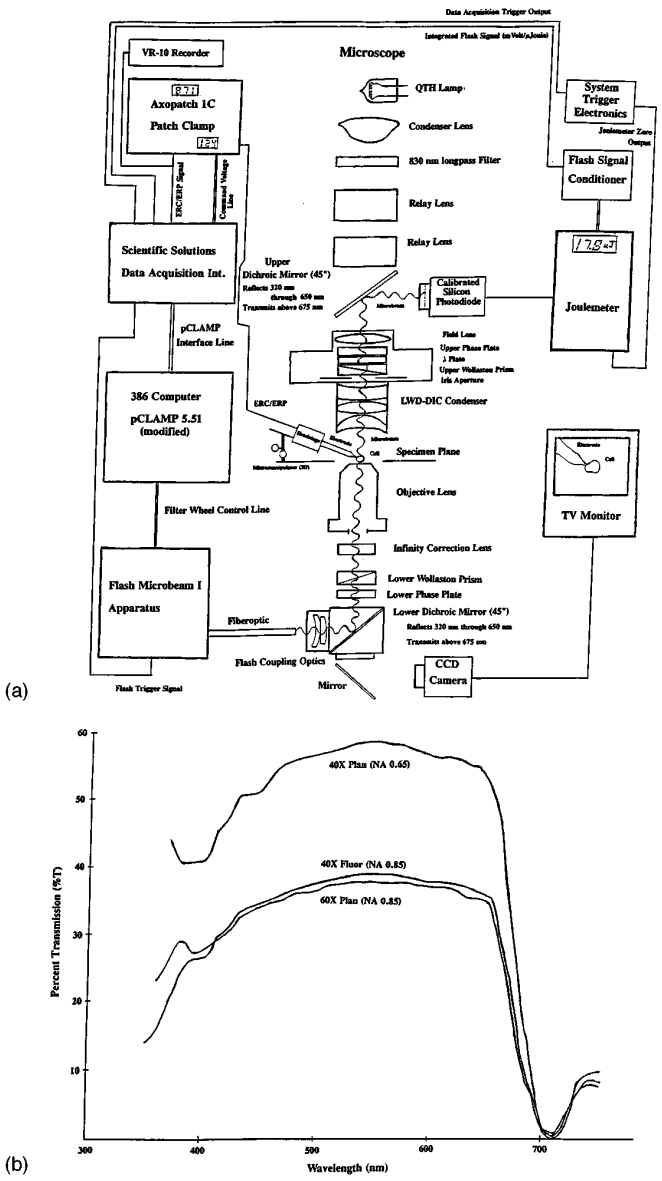

FIG. 5. Flash-by-flash measurements of microbeam Intensity. (A) An electro-optical design schematic of the electrophysiological recording and optical delivery and measurement system is shown. (B) A transmission spectrum from the specimen plane to the photodiode is shown. The light delivery system from the fiber to the specimen plane was that of Fig. 1 and its transmission spectra was shown in Fig. 3(B). The long working distance (DIC) condenser of the microscope was set up for Koehler illumination such that the specimen plane was a conjugate field plane to the field diaphragm plane. Between the condenser and the field diaphragm plane a dichroic mirror was placed that efficiently reflected ($>$98%) near-UV and visible light (320–650 nm) toward the orthogonally rotated field diaphragm plane where the calibrated photodiode was positioned in an optical mount. The photodiode sensor plane is then conjugate to the specimen field plane and can detect a large percentage of the energy of the flash in the microbeam. The spectral transmission properties between the specimen plane and photodiode were determined for three objective lenses. Percent transmission is relative to absolute photon flux delivered to the specimen plane.

bration factor and the percent optical transmission at that wavelength. The scaled joulemeter measurement then provides a measurement of the absolute microbeam flash energy in the specimen plane. This is then converted to the number of photons delivered using the energy of a single photon at a particular wavelength and Avogadro's number. The number

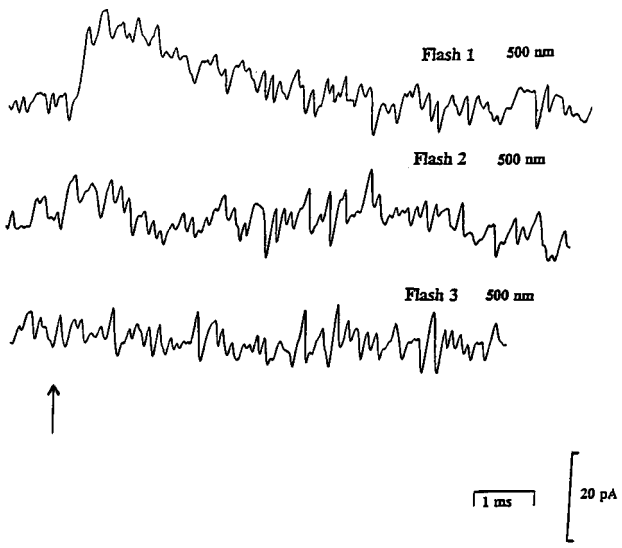

FIG. 6. ERC recordings of wild type human opsin expressed in HEK293 cells. Data are from an isolated HEK293 cell expressing wild type human rhodopsin which was subjected to WCR with routine electrophysiological buffers in the microelectrode and bath. Rhodopsin was first reconstituted with 11cRet (50 μM) for about 30 min. ERC signals were elicited using sequential 500 nm flashes ($4.2\times10(8)$ photons/μm^2) (arrow) delivered with the 40× Fluor objective. By the third flash all rhodopsin in the cell is bleached and the ERC signal is extinguished into the background whole-cell current noise.

of photons in the microbeam is then divided by the area of the spot (FWHM) in μm^2 to achieve absolute photons/μm^2 in the stimulus.

A voltage proportional to absolute photons/μm^2 can be used as an input to data acquisition systems (e.g., pCLAMP-5.51, Axon Industries) as the dependent ''light'' variable for data (e.g., ERC) acquisition. If the computer is used to control the flash wavelength, then the spectral photodiode calibration or microscope transmission scaling factors can be acquired from a look-up table. Since the spot size is a constant specified by the objective used to deliver the flash, spot diameter can also be stored for computer computation. By routing the photodiode analog flash signal into the data acquisition hardware the computer can be used to calculate absolute photons/μm^2 for each flash delivered to the preparation. A program is being developed to control all optical equipment in the system and to do these calculations to link electro-optical hardware control and flash measurement with ERC data acquisition as separate modules operative in the pCLAMP 5.51 environment. The measure of photon/μm^2 will be written as a dependent variable to the header of CLAMPEX data files during ERC recordings.

F. ERC recordings of wild type human rhodopsin

HEK293 cells expressing WT human opsin were regenerated with the native 11cRet chromophore (25–50 μM) and subjected to whole-cell recording under infared viewing conditions. A sequential series of single flashes were delivered (500 ± 35 nm) to elicit ERC currents (Fig. 6). The peak amplitude of the ERC R_2 signal and the total charge flow (integrated current) decrements with each successive flash as the amount of rhodopsin is bleached. These ERC signals recorded from human rhodopsin expressed and regenerated in HEK293 cells are similar in polarity, waveform, and time-course to whole-cell ERC signals from vertebrate rod amphibian photoreceptors[8,38] and a complete evaluation will be presented elsewhere (Sullivan, in preparation).

These results indicate that the prototype bright flash microbeam apparatus (Flash 1) delivers sufficient intensity to activate and bleach rhodopsin in single cells expressing cloned visual pigment genes. High fidelity ERC recordings can be obtained from single cells expressing less than 1 picogram of regenerable rhodopsin per cell. Moreso, ERC R_2 signals of a few milliseconds duration are commensurate with Meta-II formation, thus constituting a time-resolved study of conformational transitions in rhodopsin over this time frame (Sullivan, in preparation).

IV. DISCUSSION

A. Instrument development

A prototype bright flash microbeam device was completed to design specifications to permit the first single-cell recordings of rhodopsin activation ERC R_2 currents in a heterologous expression system containing less than 1 picogram of opsin/cell. The device delivers microbeam flashes to the specimen plane of a microscope to the order of 10^8-10^9 photons/μm^2. Flashes are band limited by selectable three-cavity interference filters. Flash duration was kept below 20 μs using a low inductance circuit layout.[59,61] The flash components are housed in a shielded box that communicates with the electrophysiological recording environment of the microscope through a high transmission efficiency fused silica fiber optic. Fiber transmission prevents the electromagnetic pulse and mechanical shock wave from the xenon plasma discharge[52,65] from reaching the electrophysiological apparatus leading to lower noise recordings from single cells without flash artifacts.

A critical initial factor in the design was the identification of the maximal fiber-optic core size that would permit high energy coupling into the rear NA of the objective lens. Clearly, larger diameter fiber optics could collect more light at the input end, but geometric factors would not permit efficient output collection to prevent severely overfilling (vignetting) the rear aperture of the objective.[62,63,66] Initial geometrical optics calculations suggested that collimation of the light source out of the fiber optic would be the most efficient way to form a microbeam without complete knowledge of the technical specifications on the objective lenses (Nikon proprietary). Once the microscope end of the system was optimized the challenge remained to couple as much light into fiber as possible. Here too, geometric constraints were relatively severe and limited consideration to the smallest (1 mm) electrode gap xenon flashlamp geometries available. The initial and excellent choice was a confined-arc bulb-type 7 J flashtube. Optical coupling of its flash into the fiber optic was relatively straightforward using fused silica optics. Xenon flashes were made monochromatic using narrow or broad band three-cavity interference filters.

All of the electronics in Flash 1 except the xenon tube power supply and the laser power supply were designed *de*

novo with the specific design needs of the instrument. Much of this design was directed toward a user friendly front panel and the ability to control the filter wheel or the flash intensity remotely using a computer. Software engineering continues to imbed control of Flash 1 and measurement of light pulses into the pCLAMP 5.51 electrophysiological data acquisition environment.

B. Comparison to other devices

This bright flash microbeam apparatus improves upon flash tube devices previously used to stimulate single-cell photolysis because of the variety of flash wavelengths which can be easily selected, the brevity of the flash durations, and the low-noise fiber-optic delivery system. Moreso, the design was accomplished with a much lower energy flash lamp and delivers comparable light intensities to other previously reported devices. Other systems had insufficient flash output or less well optimized delivery that required white flashes and back calculation of the equivalent numbers of photons in the absorbing band of the pigment under study.[8,35,37] Previous studies using xenon flashes reported long pulse durations of hundreds of microseconds[38] to milliseconds[35,37] depending upon the bulb type used, the energy of the storage system, and the inductance of the triggering/delivery network. One system used a tungsten halogen lamp and a relatively slow electromechanical shutter to deliver millisecond-order light pulses.[8] The system most similar to the prototype device developed here was that used by Makino *et al.*[38] which employed a commercially available xenon flash unit (3 mm electrode gap) mounted directly over the photoreceptor recording chamber. Individual calibrated interference filters were used to make the flashes monochromatic to the order of 10^8 photons/μm^2 in the specimen plane. The flash tube had to be mounted inside the Faraday recording cage to reach these intensities because the spot size was several millimeters in diameter. Electromagnetic pulse noise from the lamp and trigger electronics was significant and required off-line subtraction algorithms to remove it from the ERC signals prior to data analysis. Finally, no known single-cell photolysis system can measure individual flash intensities to compensate for flash-to-flash variability.

Commercially available xenon flash delivery systems are modeled after a published design.[67] These systems all appear to use a 3 mm electrode gap high pressure xenon flash tube (Model No. 35S from Chadwick Helmuth, El Monte, CA, or from Advanced Radiation Corporation, Santa Clara, CA). From optical components described in this system it is possible to calculate that the overall F/No. is about 1.0. The net optical system magnification is then about 1.0×. This means that the spot size approximates the xenon flash tube electrode gap of 3 mm and has in fact been reported at 3.6 mm diameter.[68] In this system the condenser optics were optimized to collect as much of the flash energy as possible from the xenon flash ($\approx$1.8 steradians, half angle 44.5°). However, to keep total magnification between the plasma ball and its focused image near unity a compound objective lens which generates the spot was designed with a NA of about 0.96 (F/No.$=$0.52) which corresponds to a half angle of 73°. Even though the spherical optic system generates an intense well-focused spot [Fig. 4(d)[67]], the imaging angles exceed the half-acceptance angles of liquid (0.47 NA, 56°), glass (0.56 NA, 68°), and especially fused silica (0.27 NA, 31°) fiberoptics. Thus, this system could not be used to efficiently couple into a fused silica fiber optic. In addition, the 3 mm electrode gap flash tube and the coincidently large spot size would stipulate use of a 3 mm core fiber optic which would markedly exceed the capacity of a microscope epiflourescent apparatus delivery system unless aperture limitations were imposed.[9,10] Thus, one would expect that much of the energy would not get into the fiber and the rear aperture of the objective lens would be markedly vignetted (overfilled). One would also expect that only a small fraction of the energy generated by the flash in a particular spectral band could be delivered to the specimen plane of the microscope using the same optical principles used in this system to collimate the light out of a larger diameter fiber.

In contrast, in the system developed here, the lenses used to collimate and image the flash into the fiber are optimized to match the acceptance half angle of the fiber and to keep the net transverse magnification at around 1.0. The acceptance angles of flash energy collection (0.95 steradians, 32° half cone, 0.53 NA, F/No.$=$0.94) approximated that which could be optimally delivered into the acceptance cone of the fiber (25° half cone, 0.42 NA, F/No.$=$1.2). However, the flash radiates approximately as a toroid with a 45° half angle (1.84 steradians). This system is optimized for microscope based flash delivery in that the optics were chosen to collect only that fraction of the available flash discharge which could be efficiently coupled into the 1 mm core 0.42 NA fused silica fiber optic.

The unit described delivers microbeam intensities (photons/μm^2) comparable to that seen in the larger spot diameter of Makino *et al.*[38] but without the noise associated with xenon plasma ignition because of fiber-optic delivery. Makino *et al.*[38] used the 35S flash tube and delivered the flash into an approximately 3 mm spot diameter in the specimen plane. The capacitor discharged 300 J into the lamp compared to the 7 J delivered in this system. This highlights the efficiency of the system reported here. This unit delivers equivalent flash intensities, even with a xenon bulb of considerably lower energy ($\approx$2%), because of a carefully constrained geometrical design. From the first principles the fiber-optic core size was chosen to maximize filling of the rear aperture of the objective lens condensers without significant vignetting. The optics in the epifluorescent port serve only to collimate and limit divergence of the beam out of the fiber. At the input end of the fiber an $\approx$F/No.1 optical delivery system was chosen to maximize coupling of the flash originating from a small plasma ball between the xenon flash tube electrodes (1 mm) into the 1 mm core fiber optic. The optical design at the input end of the fiber efficiently collected only as much of the flash tube output as would efficiently fill the collection cone of the NA 0.42 fused silica fiber optic. There is no net transverse optical magnification in the delivery system which would only have led to vignetting of the fiber input face, or larger beams presented to the objective rear aperture. Both effects would have decreased

throughput to the specimen plane. The optical result is that the plasma ball between the flash tube electrodes is a conjugate field plane with the microscope specimen plane.

We have demonstrated that a careful geometric optical design can achieve equivalent flash intensity in microbeams as are generated with considerably more powerful xenon lamp discharges and consequently larger spot sizes. In addition the pulse duration is 14 μs at full capacitor charge. The pulse duration in the Makino *et al.*[38] study was several hundred microseconds. Thus, the choice of flash tube, and the electrical and optical delivery systems are much more well optimized, given that equivalent light intensities can be obtained with a 7 J flash tube compared to a 300 J flash tube even while the flash pulse duration was minimized by at least an order of magnitude. This system permits much more efficient intense flash delivery to single cells viewed microscopically and without additional noise sources to electrophysiological recording hardware.

C. Utility of the instrument

This device was used to stimulate rhodopsin ERCs from expressed pigment in cultured cells, but could be used identically to stimulate rhodopsin activation in single photoreceptors. It would have nearly equal facility to stimulate both rod or cone visual pigments which have similar photosensitivities. Using different condensers at the output of the fiber to replace the objective lens it could be used to stimulate rhodopsin ERCs in Xenopus oocytes expressing rhodopsin[69] or in artificial membrane bilayer preparations in which rhodopsin or other pigments are oriented.[70–72] In the context of photoreceptor physiology, this device has significant use in studies of activation of the transduction apparatus by Meta-II and can be used to evaluate photoreversal effects.[47,48] Since Meta-II (peak absorption 380 nm) has a several minute lifetime at room temperature, it should be feasible to photoconvert it back toward rhodopsin using high near-UV intensity flashes prior to hydrolysis of the deprotonated Schiff base linkage. Since the flash intensity can be linearly regulated by steady voltage input levels to the flash power supply, photoreceptor responses to a programmed series of incrementing flash intensities can be studied.

The device has broader applications to studies requiring activation or photolysis of any type of cellular pigment in which the extinction coefficient is at least moderately high. The device has potential applicability as a caged-compound photolysis unit to liberate biologically active compounds from their inactive but light-sensitive precursor molecules.[9,68,73–75] Preliminary calculations indicate that Flash 1 could be used as a caged compound liberation device for single cells loaded with such agents (e.g., 250 μM) using patch clamp pipettes. The unit as currently constructed could potentially release low micromolar concentrations of caged compounds with moderately high extinction coefficients (e.g., 5000 $M^{-1}\,cm^{-1}$) in a single flash. Concentration increases could be enhanced by the rapid delivery of a preprogrammed series of identical flashes which this instrument can already deliver using the count-to-N-and-stop trigger. However, microbeam intensities will need to be greater for high efficacy liberation of caged compounds with lower extinction coefficients in single brief flashes. Several engineering modifications are being evaluated to further enhance single flash microbeam intensities to expand the potential uses of this device (Sullivan, work in progress).

V. DISCUSSION

A novel bright flash microbeam apparatus has been designed, fabricated, tested, and calibrated and will serve as a novel tool to explore charge mobilization in rhodopsin during conformational transitions. The unit is versatile, however, and could find use in any application requiring photolysis of pigments in single cells. The device achieves high microbeam intensity because of a very careful optical design and component selection. All critical optical and electronic components are commercially available. A xenon flash system was chosen on the basis of cost; a N_2-dye laser would have been used but would have cost in the vicinity of $30K. To avoid electromagnetic noise due to xenon flash tube discharge the flash apparatus was housed in a double Faraday cage and the light pulse was commutated to the Nikon Diaphot microscope using a two meter long fused silica core fiber optic. The instrument operates to design specifications and has already demonstrated utility in activating conformational activation currents from single cells expressing less than 1 picogram of human rhodopsin. Time-resolved spectroscopic studies of rhodopsin require at a minimum tens of micrograms (electron spin resonance) and often tens of milligrams (absorption, Fourier transform infrared) of regenerated visual pigment. These levels are currently difficult at best if not impossible to achieve from standard cellular expression systems. The use of this flash apparatus has demonstrated that the ERC can be used as a time-resolved tool to study rhodopsin activation with at least 10^7 fold greater sensitivity than with other methods and with microsecond order time resolution. The sensitivity of this method should markedly assist in structure-function analyses of mutant rhodopsins that are difficult to express in large quantities.[22,23] In addition these tools allow exploration of the biophysical processes that control rhodopsin activation (Sullivan, work in progress).

ACKNOWLEDGMENTS

The author would like to thank Eric Arnold (Dept. of Ophthalmology, University of Michigan) for his assistance with *de novo* electronic designs and for providing the filter wheel positioning module. This project benefited significantly from discussions with Dr. Gordon Ellis and Robert Knudson (Technical Video Ltd., Woods Hole, MA) about fiber optic coupling to microscopes. The author acknowledges the assistance of Randall Zywicki with the optical energy throughput calculations. The author would like to thank Bob Capobianco and Jim Collis of EG&G who provided parts, specifications and experience with xenon flash tubes and triggering configurations. In addition this project was greatly assisted by technical data on the microscope and objective lenses provided by the Nikon Corporation. The author thanks Dr. Jeremy Nathans for providing the wild type hu-

man opsin expressing cell line and Dr. Gary Trick for the use of his monochromators. This work was funded by the Foundation Fighting Blindness during a Career Development Award (J.M.S.), a Heed/Knapp Foundation grant (J.M.S.), a CORE grant to the Department of Ophthalmology at the University of Michigan (EY07003), and a National Eye Institute First Award (J.M.S.) (EY11384).

[1] S. Zamenhof, Rev. Sci. Instrum. **14**, 17 (1943).
[2] R. B. Uretz and R. P. Perry, Rev. Sci. Instrum. **28**, 861 (1957).
[3] M. W. Berns, J. Aist, J. Edwards, K. Strahs, J. Girton, P. McNeill, J. B. Rattner, M. Kitzes, M. Hammer-Wilson, L.-H. Liaw, A. Siemens, M. Koonce, S. Peterson, S. Brenner, J. Burt, R. Walter, P. J. Bryant, D. van Dyk, J. Coulombe, T. Cahill, and G. S. Berns, Science **213**, 505 (1981).
[4] R. J. Leslie and J. D. Pickett-Heaps, J. Cell Biol. **96**, 548 (1983).
[5] P. Wilson and A. Forer, Biochem. Cell Biol. **65**, 363 (1987).
[6] O. G. Stonington, T. P. Spurck, J. A. Snyder, and J. D. Pickett-Heaps, Protoplasma **153**, 62 (1989).
[7] W. Stuhmer and W. Almers, Proc. Natl. Acad. Sci. USA **79**, 946 (1982).
[8] S. Hestrin and J. I. Korenbrot, J. Neurosci. **10**, 1967 (1990).
[9] E. Niggli and W. J. Lederer, Biophys. J. **59**, 1123 (1991).
[10] M. S. Kirby, R. W. Hadley, and W. J. Lederer, Pflugers Arch. Ges. Physiol. Menschen Tiere **427**, 169 (1994).
[11] D. Bownds, Nature (London) **216**, 1178 (1967).
[12] O. P. Hamill, A. Marty, E. Neher, B. Sakmann, and F. J. Sigworth, Pflugers Arch. Ges. Physiol. Menschen Tiere **391**, 85 (1981).
[13] H. J. A. Dartnall, Br. Med. Bull. **9**, 24 (1953).
[14] A. Kropf, Vision Res. **7**, 811 (1967).
[15] R. W. Schoenlein, L. A. Peteanu, R. A. Mathies, and C. V. Shank, Science **254**, 412 (1991).
[16] R. R. Birge, C. M. Einterz, H. M. Knapp, and L. P. Murray, Biophys. J. **53**, 367 (1988).
[17] J. H. Parkes and P. A. Liebman, Biochemistry **23**, 5054 (1984).
[18] C. Longstaff, R. Calhoon, and R. A. Rando, Proc. Natl. Acad. Sci. USA **83**, 4209 (1986).
[19] A. A. Lamola, T. Yamane, and A. Zipp, Biochemistry **13**, 738 (1974).
[20] D. S. Cafiso and W. L. Hubbell, Biophys. J. **30**, 243 (1980).
[21] J. Nathans, C. J. Weitz, N. Agarwal, I. Nir, and D. S. Papermaster, Vision Res. **29**, 907 (1989).
[22] C.-H. Sung, B. G. Schneider, N. Agarwal, D. S. Papermaster, and J. Nathans, Proc. Natl. Acad. Sci. USA **88**, 8840 (1991).
[23] C.-H. Sung, C. M. Davenport, and J. Nathans, J. Biol. Chem. **268**, 26645 (1993).
[24] K. Fahmy, F. Jager, M. Beck, T. A. Zvyaga, and T. P. Sakmar, Proc. Natl. Acad. Sci. USA **90**, 10206 (1993).
[25] P. Rath, L. L. J. DeCaluwe, P. H. M. Bovee-Geurts, W. J. DeGrip, and K. J. Rothschild, Biochemistry **32**, 10277 (1993).
[26] J. W. Lewis, F. J. G. M. van Kuijk, T. E. Thorgeirsson, and D. S. Kliger, Biochemistry **30**, 11372 (1991).
[27] O. Kuwata, C. Yuan, and T. G. Ebrey, Invest. Ophthalmol. Visual Sci. **38**, 593S (1997).
[28] G. B. Cohen, D. D. Oprian, and P. R. Robinson, Biochemistry **31**, 12592 (1992).
[29] C. J. Weitz and J. Nathans, Biochemistry **32**, 14176 (1993).
[30] S. Arnis, K. Fahmy, K. P. Hofmann, and T. P. Sakmar, J. Biol. Chem. **269**, 23879 (1994).
[31] H. W. Trissl, Biophys. Struct. Mech. **8**, 213 (1982a).
[32] J. D. Spalink and H. Stieve, Biophys. Struct. Mech. **6**, 171 (1980).
[33] P. Hochstrate, M. Lindau, and H. Ruppel, Biophys. J. **38**, 53 (1982).
[34] H. W. Trissl, Mtds. Enzymol. **81**, 431 (1982b).
[35] J. E. Lisman and H. Bering, J. Gen. Physiol. **70**, 621 (1977).
[36] T. G. Ebrey, Vision Res. **8**, 965 (1968).
[37] A. L. Hodgkin and P. M. O'Bryan, J. Physiol. (London) **267**, 737 (1977).
[38] C. L. Makino, W. R. Taylor, and D. A. Baylor, J. Physiol. (London) **442**, 761 (1991).
[39] R. A. Cone, Science **155**, 1128 (1967).
[40] R. A. Cone, Exp. Eye Res. **8**, 246 (1969).
[41] R. A. Cone and W. L. Pak, in *Handbook of Sensory Physiology: Principles of Receptor Physiology*, edited by W. R. Lowenstein (Springer, Berlin, 1971), Vol. 1, Chap. 12, pp. 345–365.
[42] F. Bezanilla and E. Stefani, Annu. Rev. Biophys. Biomol. Struct. **23**, 819 (1994).
[43] H. W. Trissl, Photochem. Photobiol. **29**, 579 (1979).
[44] L. A. Drachev, G. R. Kalamkarov, A. D. Kaulen, M. A. Ostrovsky, and V. P. Skulachev, Eur. J. Biochem. **117**, 471 (1981).
[45] T. P. Williams, J. Gen. Physiol. **47**, 679 (1964).
[46] T. P. Williams, Vision Res. **5**, 633 (1965).
[47] E. N. Pugh, Jr., J. Physiol. (London) **248**, 393 (1975a).
[48] E. N. Pugh, Jr., J. Physiol. (London) **248**, 413 (1975b).
[49] W. Ernst and C. M. Kemp, Vision Res. **19**, 363 (1979).
[50] S. Inoue, *Video Microscopy* (Plenum, New York, 1986), pp. 93–148.
[51] A. C. Hardy and F. M. Young, J. Opt. Soc. Am. **39**, 265 (1949).
[52] J. H. Goncz, J. Appl. Phys. **36**, 742 (1965).
[53] J. H. Goncz and P. B. Newell, J. Opt. Soc. Am. **56**, 87 (1962).
[54] M. A. Gusinow, J. Appl. Phys. **44**, 4567 (1973).
[55] M. A. Gusinow, J. Appl. Phys. **46**, 4847 (1975).
[56] H. E. Edgerton, R. Bonazoli, and J. T. Lamb, J. SMPTE **63**, 15 (1954).
[57] H. E. Edgerton, J. H. Goncz, and P. W. Jameson, in *Proceedings of the Sixth International Congress on High-Speed Photography*, edited by J. G. A. deGraaf and P. Tegelaar (H. D. Tjeenk Willink & Zoon N. V., Haarlem, 1963), pp. 143–151.
[58] A. Buck, R. Erickson, and F. Barnes, J. Appl. Phys. **34**, 2115 (1963).
[59] J. P. Markiewicz and J. L. Emmett, J. Quantum Electron. **QE-2**, 707 (1966).
[60] D. E. Perlman, Rev. Sci. Instrum. **37**, 340 (1966).
[61] T. Efthymiopoulos and B. K. Garside, Appl. Opt. **16**, 70 (1977).
[62] G. W. Ellis, J. Cell Biol. **83**, 303a (1979).
[63] G. W. Ellis, J. Cell Biol. **101**, 83a (1985).
[64] H. J. A. Dartnall, Vision Res. **8**, 339 (1968).
[65] G. W. LeCompte and H. E. Edgerton, J. Appl. Phys. **27**, 1427 (1956).
[66] R. A. Knudson, Am. Lab. June, 50 (1990).
[67] G. Rapp and K. Guth, Pflugers Arch. Ges. Physiol. Menschen Tiere **411**, 200 (1988).
[68] J. M. Nerbonne, in *Optical Methods in Cell Physiology*, edited by P. DeWeer and B. M. Salzberg (Wiley, New York, 1986), Vol. 40, Society of General Physiologists Series, Chap. 24, pp. 417–445.
[69] H. G. Khorana, B. E. Knox, E. Nasi, R. Swanson, and D. A. Thompson, Proc. Natl. Acad. Sci. USA **85**, 7917 (1988).
[70] H. W. Trissl, A. Darszon, and M. Montal, Proc. Natl. Acad. Sci. USA **74**, 207 (1977).
[71] M. Lindau, P. Hochstrate, and H. Ruppel, FEBS Lett. **112**, 17 (1980).
[72] J. S. Huebner, R. T. Arrieta, I. C. Arrieta, and P. M. Pachori, Photochem. Photobiol. **39**, 191 (1984).
[73] H. A. Lester, L. D. Chabala, A. M. Gurney, and R. E. Sheridan, in *Optical Methods in Cell Physiology*, edited by P. DeWeer and B. M. Salzberg (Wiley, New York, 1986), Vol. 40, Society of General Physiologists Series, Chap. 25, pp. 448–462.
[74] J. H. Kaplan and A. P. Somlyo, TINS **12**, 54 (1989).
[75] J. A. McCray and D. R. Trentham, Annu. Rev. Biophys. Biophys. Chem. **18**, 239 (1989).